

Received July 11, 2019, accepted July 28, 2019, date of publication July 31, 2019, date of current version August 15, 2019.

Digital Object Identifier 10.1109/ACCESS.2019.2932261

# Adaptive Robust Cubature Kalman Filter for Power System Dynamic State Estimation Against Outliers

YI WANG<sup>1,2</sup>, (Student Member, IEEE), YONGHUI SUN<sup>1</sup>, (Member, IEEE),  
VENKATA DINAHAH<sup>2</sup>, (Senior Member, IEEE), SHIQI CAO<sup>2</sup>, (Student Member, IEEE),  
AND DONGCHEN HOU<sup>1</sup>

<sup>1</sup>College of Energy and Electrical Engineering, Hohai University, Nanjing 210098, China

<sup>2</sup>Department of Electrical and Computer Engineering, University of Alberta, Edmonton, AB T6G 2V4, Canada

Corresponding author: Yonghui Sun (sunyonghui168@gmail.com)

This work was supported in part by the National Natural Science Foundation of China under Grant 61673161, in part by the Natural Science Foundation of Jiangsu Province of China under Grant BK20161510, in part by the Six Talent Peaks High Level Project of Jiangsu Province under Grant 2017-XNY-004, and in part by the Natural Science and Engineering Research Council (NSERC) of Canada. The work of Y. Wang was supported by the China Scholarship Council.

**ABSTRACT** This paper develops an adaptive robust cubature Kalman filter (ARCKF) that is able to mitigate the adverse effects of the innovation and observation outliers while filtering out the system and measurement noises. To develop the ARCKF dynamic state estimator, a batch-mode regression form in the framework of cubature Kalman filter is first established by processing the predicted state and measurement data information simultaneously. Subsequently, based on the regression form, the outliers can be detected and downweighted by the robust projection statistics approach. Then, the adverse effects of innovation and observation outliers can be effectively suppressed by the generalized maximum likelihood (GM)-type estimator utilizing the iteratively reweighted least squares approach. Finally, an adaptive strategy is developed to adjust the state estimation error covariance matrix under different conditions. Extensive simulation results obtained from the IEEE New England 10-machine 39-bus test system under various operating conditions demonstrate the effectiveness and robustness of the proposed method, which is able to track the transients of power system in a more reliable way than the conventional cubature Kalman filter (CKF) and the unscented Kalman filter (UKF).

**INDEX TERMS** Dynamic state estimation, cubature Kalman filter, robust estimation, outliers, power system stability.

## I. INTRODUCTION

Accurate and reliable dynamic state estimator (DSE) is gradually becoming more and more important for the secure and stable operation of power systems, since it can provide the essential information for power system real-time monitoring and control [1]–[5]. To cite a few, in [6], based on the estimated results of generator's angle, a modified out-of-step detection approach for generators was proposed. On the other hand, in [7], the dynamic state estimation results were leveraged for the design of series compensated transmission line protection. These wide ranging applications of DSE have

The associate editor coordinating the review of this manuscript and approving it for publication was Padmanabh Thakur.

effectively enhanced the stability and reliability of power system.

The dynamic state variables of power system can be estimated in real-time by utilizing the measurement data from high-level phasor measurement units (PMUs) [8]. To date, for effectively tracking power system dynamics, various DSEs have been proposed and investigated in [11]–[15]. For instance, by utilizing the available measurement data measured by PMUs, the DSE based on Kalman filter (KF) methods were investigated in [9] and [10]. Following their work, in [11], a modified extended Kalman filter was proposed. In [12], by assuming the mechanical torque is known, the work of [11] was further extended to a decentralized DSE, which only requires the local

measurement information. However, due to the first-order approximation errors in the linearized process of nonlinear function, EKF method could only be utilized for a mild nonlinear system [13]. To circumvent the linearization errors of EKF, by utilizing the multi-step adaptive interpolation technique, an improved EKF method that enhanced the state estimation accuracy to a certain extent was proposed in [14]. Moreover, in [15], an extended particle filter was proposed which leveraged the Monte Carlo simulation to propagate the mean and covariance matrices of states, thus a much better state estimation accuracy than the EKF approach could be obtained. In addition, some derivative-free Kalman filters based DSE were also proposed to achieve more accurate system monitoring, such as the unscented Kalman filter [16]–[18] and the cubature Kalman filter [19], [20].

These previous efforts have greatly promoted the level of power system monitoring undoubtedly. However, it should be noted that all the aforementioned methods work well only when some assumptions are satisfied [21], [22]. First, the measurements are assumed to be obtained accurately without any large deviations. Second, both the system and measurement noise are assumed to be Gaussian [23]. In fact, for a practical power system, either assumption can be often violated due to the existence of observation and innovation outliers. Therefore, as demonstrated in [24], the performance of conventional Kalman-type filters is degraded sharply in the presence of outliers due to their lack of robustness.

In general, for an actual power system, the observation outliers can arise from the biases in PMU measurements that are mainly caused by instrument failures, impulsive communication noise or infrequent calibration [25]. Therefore, the observation outliers seriously affect the measured value. As for the innovation outliers, they are often introduced by the undesirable system process impulsive noise or inaccurate approximations in the state prediction model, which might corrupt the predicted state estimates. To address these issues, some robust dynamic state estimation methods were proposed. Specifically, by utilizing the least absolute value estimator, a robust distributed DSE against observation outliers was developed in [26]. However, the vulnerability of DSE to innovation outliers is not tackled. Then, in order to mitigate the adverse effects of observation and innovation outliers, a robust iterated extended Kalman filter was developed in [24], but it may suffer from the divergence problem while the system model exhibits strong nonlinearity. As a result, significantly biased estimation results might be obtained. To deal with this problem, a modified UKF approach was proposed in [27] that just expanding their own work in the similar structure of [24]. However, it is worth pointing out that the convergence of this method may be affected by the sampling methods of Sigma points and is not quite suitable for the high dimension system [28]. More importantly, the calculation of its state estimation covariance matrix may be too conservative, where too much emphasis was placed in accommodating the worst case at the expense of optimality.

To deal with the aforementioned challenges, by resorting to robust statistics, this paper develops an adaptive robust cubature Kalman filter that is able to suppress the outliers and achieve a high estimation accuracy. At first, a batch-mode regression form is introduced to enhance the measurement data redundancy. Subsequently, based on the regression form, the robust projection statistics approach is introduced to detect and downweight the outliers. Then, the robust GM-estimator is utilized to mitigate the adverse effects of outliers. Finally, an adaptive strategy is proposed to adjust the state estimation error covariance matrix under various conditions, which can balance the robustness and accuracy of the proposed method.

The remainder of this paper is organized as follows. In Section II, the state-space model for tracking power system state dynamics is established and presented. In Section III, the proposed ARCKF method is developed and introduced in detail. In Section IV, extensive simulations are carried out on the IEEE 10-machine 39-bus test system to demonstrate the efficacy of the proposed method, and finally the conclusions are drawn in Section V.

## II. DYNAMIC STATE ESTIMATION MODEL

In this part, based on the fourth order transient generator model and the modified Euler approach [29], the discrete-time state-space model of a synchronous generator for tracking the state dynamics is presented.

### A. FOURTH ORDER TRANSIENT MODEL

For a synchronous generator, the 4<sup>th</sup> order differential equations in the local  $d - q$  reference frame can be expressed as follows [14], [30]

$$\begin{cases} \frac{d\delta}{dt} = \omega - \omega_0 \\ \frac{d\omega}{dt} = \frac{\omega_0}{2H} \left( T_m - T_e - \frac{K_D}{\omega_0} (\omega - \omega_0) \right) \\ \frac{de'_q}{dt} = \frac{1}{T'_{d0}} \left( E_{fd} - e'_q - (x_d - x'_d) i_d \right) \\ \frac{de'_d}{dt} = \frac{1}{T'_{q0}} \left( -e'_d + (x_q - x'_q) i_q \right), \end{cases} \quad (1)$$

where  $\delta$  denotes the rotor angles;  $\omega$  denotes the rotor speeds in per-unit,  $\omega_0 = 2\pi f_0$  represents the rated value of the angular frequency;  $H$  and  $K_D$  are respectively the inertia constant and the damping factor; the parameters  $T_m$  and  $T_e$  represent the mechanical torque and the electric air-gap torque, respectively;  $E_{fd}$  indicates the internal field voltage; the variables  $e'_d$  and  $e'_q$  denote the transient voltages along the local  $d$  and  $q$  axes, respectively; the parameters  $T'_{d0}$  and  $T'_{q0}$  indicate the open circuit time constants along the directions of  $d$  and  $q$  axes, respectively;  $x_d$  and  $x_q$  are respectively the synchronous reactance along  $d$  and  $q$  axes, respectively;  $x'_d$  and  $x'_q$  are the associated transient reactance at  $d$  and  $q$  axes, respectively;  $i_d$  and  $i_q$  are the stator currents in the directions of  $d$  and  $q$  axes, respectively.

For the sake of notation, (1) can be rewritten as a general state-space form

$$\begin{cases} \dot{\mathbf{x}} = \mathbf{f}_c(\mathbf{x}, \mathbf{u}) + \mathbf{w}_c \\ \mathbf{y} = \mathbf{h}_c(\mathbf{x}, \mathbf{u}) + \mathbf{v}_c, \end{cases} \quad (2)$$

where  $c$  represents the continuous-time model,  $\mathbf{x}$  denotes the state vector that consist of  $\omega$ ,  $\delta$ ,  $e'_d$  and  $e'_q$ ;  $\mathbf{f}_c(\cdot)$  indicates the nonlinear state transition function,  $\mathbf{h}_c(\cdot)$  is the measurement function;  $\mathbf{w}_c$  and  $\mathbf{v}_c$  are respectively the process and measurement noise, which are usually assumed to be Gaussian white noise with covariance matrices  $\mathbf{Q}$  and  $\mathbf{R}$ , respectively; the input vector  $\mathbf{u}$  and the output vector  $\mathbf{y}$  are respectively [30]

$$\mathbf{u} = [T_m \quad E_{fd} \quad i_R \quad i_I]^T, \quad (3)$$

$$\mathbf{y} = [\delta \quad \omega \quad e_R \quad e_I]^T, \quad (4)$$

where  $i_R$  and  $i_I$  represent the stator currents along the  $R$  and  $I$  axes,  $e_R$ ,  $e_I$  are the associated stator voltages.

To transform (1) into the state transition function  $\mathbf{f}_c(\cdot)$  in (2),  $i_d$ ,  $i_q$  and  $T_e$  need to be written as functions of  $\mathbf{x}$  and  $\mathbf{u}$  utilizing (5)-(7)

$$i_d = i_R \sin \delta - i_I \cos \delta, \quad (5)$$

$$i_q = i_I \sin \delta + i_R \cos \delta, \quad (6)$$

$$T_e = (e'_d + i_q x'_d) i_d + (e'_q - i_d x'_d) i_q. \quad (7)$$

Similarly, to implement the measurement function  $\mathbf{h}_c(\cdot)$  in (2),  $e_R$  and  $e_I$  need to be written as functions of  $\mathbf{x}$  and  $\mathbf{u}$  using (8)

$$\begin{bmatrix} e_R \\ e_I \end{bmatrix} = \begin{bmatrix} \sin \delta & \cos \delta \\ -\cos \delta & \sin \delta \end{bmatrix} \begin{bmatrix} e'_d \\ e'_q \end{bmatrix} - \begin{bmatrix} \cos \delta & -\sin \delta \\ \sin \delta & \cos \delta \end{bmatrix} \begin{bmatrix} x'_d i_d \\ x'_q i_q \end{bmatrix}. \quad (8)$$

### B. DISCRETE STATE-SPACE MODEL

Similar to [30], to track the dynamic state variables of generators utilizing the measurements, the continuous system model in (2) needs to be further discretized into the discrete form

$$\begin{cases} \mathbf{x}_k = \mathbf{f}(\mathbf{x}_{k-1}, \mathbf{u}_{k-1}) + \mathbf{w}_{k-1} \\ \mathbf{y}_k = \mathbf{h}(\mathbf{x}_k, \mathbf{u}_k) + \mathbf{v}_k, \end{cases} \quad (9)$$

where  $k$  indicates the time instant at  $k \Delta t$ , and  $\Delta t$  represents the sampling interval;  $\mathbf{w}_k$  and  $\mathbf{v}_k$  are the process and measurement noise with covariance matrices  $\mathbf{Q}_k$  and  $\mathbf{R}_k$ , respectively.

To be specific, the state transition function  $\mathbf{f}_c(\cdot)$  is discretized by applying the modified Euler technique [29]

$$\tilde{\mathbf{x}}_k = \mathbf{x}_{k-1} + \mathbf{f}_c(\mathbf{x}_{k-1}, \mathbf{u}_{k-1}) \Delta t, \quad (10)$$

$$\tilde{\mathbf{f}} = \frac{\mathbf{f}_c(\tilde{\mathbf{x}}_k, \mathbf{u}_k) + \mathbf{f}_c(\mathbf{x}_{k-1}, \mathbf{u}_{k-1})}{2}, \quad (11)$$

$$\mathbf{x}_k = \mathbf{x}_{k-1} + \tilde{\mathbf{f}} \Delta t, \quad (12)$$

and the measurement function  $\mathbf{h}_c(\cdot)$  can be directly discretized as follows

$$\mathbf{y}_k = \mathbf{h}_c(\mathbf{x}_k, \mathbf{u}_k) + \mathbf{v}_k. \quad (13)$$

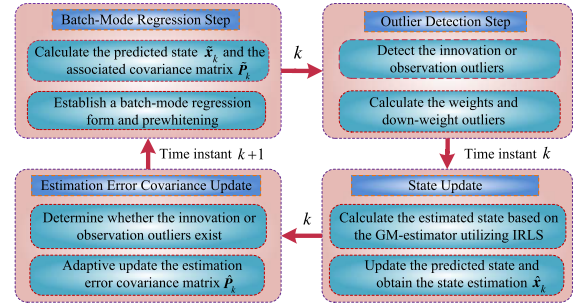


FIGURE 1. Framework of the proposed ARCKF method.

Based on the received measurements at each time instant, the discrete state-space model expressed in (9) can be utilized to track the state dynamics of power system.

### III. PROPOSED ARCKF METHOD

In this section, the proposed ARCKF method is developed and its overall framework can be found in Fig. 1.

#### A. DERIVATION OF THE BATCH-MODE REGRESSION FORM

##### 1) CUBATURE POINT GENERATION

Given the estimated state vector  $\hat{\mathbf{x}}_{k-1} \in \mathbb{R}^{n \times 1}$  and the corresponding state estimation error covariance matrix  $\hat{\mathbf{P}}_{k-1} \in \mathbb{R}^{n \times n}$  at time instant  $k - 1$ ,  $2n$  cubature points that capture the statistical properties of  $\hat{\mathbf{x}}_{k-1}$  can be generated [19], [20]. Formally, we get

$$\mathbf{X}_{i,k-1} = \hat{\mathbf{x}}_{k-1} + \xi_i \sqrt{\hat{\mathbf{P}}_{k-1}}, \quad i = 1, \dots, 2n \quad (14)$$

where  $\mathbf{X}_{i,k-1}$  is the  $i$  th cubature point of  $\hat{\mathbf{x}}_{k-1}$ ,  $n$  indicates the dimension of state variable,  $\sqrt{\cdot}$  represents the operation of Cholesky decomposition,  $\xi_i$  denotes the  $i$  th column of the basic data point set that defined as follows

$$\xi_i = \begin{cases} \sqrt{n}[\mathbf{e}]_i, & i = 1 \dots n \\ -\sqrt{n}[\mathbf{e}]_{i-n}, & i = n + 1 \dots 2n, \end{cases} \quad (15)$$

where  $\mathbf{e}$  represents a unity matrix of size  $n \times n$ .

##### 2) STATE PREDICTION

Here, the cubature points are instantiated via the state transition function  $\mathbf{f}(\cdot)$  in (9). Then, the predicted state and the associated state error covariance can be calculated by

$$\mathbf{X}_{i,k}^* = \mathbf{f}(\mathbf{X}_{i,k-1}, \mathbf{u}_{k-1}), \quad i = 1, \dots, 2n \quad (16)$$

$$\tilde{\mathbf{x}}_k = \frac{1}{2n} \sum_{i=1}^{2n} \mathbf{X}_{i,k}^*, \quad (17)$$

$$\tilde{\mathbf{P}}_k = \frac{1}{2n} \sum_{i=1}^{2n} \mathbf{X}_{i,k}^* (\mathbf{X}_{i,k}^*)^T - \tilde{\mathbf{x}}_k \tilde{\mathbf{x}}_k^T + \mathbf{Q}_{k-1}, \quad (18)$$

where  $\mathbf{X}_{i,k}^*$  indicates the transformed cubature points,  $\tilde{\mathbf{x}}_k$  is the predicted state,  $\tilde{\mathbf{P}}_k$  is the corresponding error covariance, the superscript  $T$  represents the matrix transpose operation.

### 3) REGRESSION FORM CONSTRUCTION

To construct the batch-mode regression form, the relation between the predicted state  $\tilde{\mathbf{x}}_k$  and the true state  $\mathbf{x}_k$  is utilized [27]

$$\tilde{\mathbf{x}}_k = \mathbf{x}_k - \boldsymbol{\eta}_k, \quad (19)$$

where  $\boldsymbol{\eta}_k$  represents the prediction error.

In addition, by applying the statistical linearization technique [31] to the measurement function  $\mathbf{h}(\cdot)$  at  $\tilde{\mathbf{x}}_k$ , the following can be derived

$$\mathbf{y}_k = \mathbf{H}_k (\mathbf{x}_k - \tilde{\mathbf{x}}_k) + \mathbf{h}(\tilde{\mathbf{x}}_k) + \mathbf{v}_k, \quad (20)$$

where  $\mathbf{H}_k = (\mathbf{P}_{xy,k})^T (\tilde{\mathbf{P}}_k)^{-1}$  represents the statistical regression matrix, and the cross covariance matrix  $\mathbf{P}_{xy,k}$  can be calculated by

$$\tilde{\mathbf{y}}_k = \frac{1}{2n} \sum_{i=1}^{2n} \mathbf{Y}_{i,k}, \quad (21)$$

$$\mathbf{P}_{xy,k} = \frac{1}{2n} \sum_{j=1}^{2n} \mathbf{X}_{i,k}^* \mathbf{Y}_{i,k}^T - \tilde{\mathbf{x}}_k \tilde{\mathbf{y}}_k^T, \quad (22)$$

where  $\mathbf{Y}_{i,k} = \mathbf{h}(\mathbf{X}_{i,k}^*)$ ,  $i = 1, \dots, 2n$ .

Then, (19) and (20) can be written into a matrix form as follows

$$\begin{bmatrix} \mathbf{y}_k + \mathbf{H}_k \tilde{\mathbf{x}}_k - \mathbf{h}(\tilde{\mathbf{x}}_k) \\ \tilde{\mathbf{x}}_k \end{bmatrix} = \begin{bmatrix} \mathbf{H}_k \\ \mathbf{I} \end{bmatrix} \mathbf{x}_k + \begin{bmatrix} \mathbf{v}_k \\ -\boldsymbol{\eta}_k \end{bmatrix}, \quad (23)$$

which can be further rewritten as a compact form

$$\tilde{\mathbf{Y}}_k = \tilde{\mathbf{H}}_k \mathbf{x}_k + \tilde{\boldsymbol{\epsilon}}_k, \quad (24)$$

where the covariance matrix of  $\tilde{\boldsymbol{\epsilon}}_k$  can be derived as follows

$$\boldsymbol{\Sigma}_k = \mathbb{E}[\tilde{\boldsymbol{\epsilon}}_k \tilde{\boldsymbol{\epsilon}}_k^T] = \begin{bmatrix} \mathbf{R}_k & \mathbf{0} \\ \mathbf{0} & \tilde{\mathbf{P}}_k \end{bmatrix} = \mathbf{S}_k \mathbf{S}_k^T, \quad (25)$$

where  $\mathbf{S}_k$  can be calculated by the UD factorization or the Cholesky decomposition technique [32].

Finally, the  $\tilde{\boldsymbol{\epsilon}}_k$  needs to be prewhitened [32], which can be realized by multiplying  $\mathbf{S}_k^{-1}$  on the both sides of (24), yielding

$$\mathbf{S}_k^{-1} \tilde{\mathbf{Y}}_k = \mathbf{S}_k^{-1} \tilde{\mathbf{H}}_k \mathbf{x}_k + \mathbf{S}_k^{-1} \tilde{\boldsymbol{\epsilon}}_k, \quad (26)$$

which can be expressed in a compact form as

$$\mathbf{z}_k = \mathbf{C}_k \mathbf{x}_k + \boldsymbol{\zeta}_k. \quad (27)$$

*Remark 1:* In this part, by utilizing the statistical linearization approach [31], a batch-mode regression form in the framework of CKF was firstly developed by processing the predicted state and measurement data information simultaneously, resulting an enhanced measurement data redundancy. This measurement data redundancy is very important and necessary for our estimator to mitigate the adverse effects of the innovation and observation outliers. In addition, it is worth pointing out that the designed batch-mode regression form inherits the benefits of CKF, which can give a systematic solution for high-dimensional nonlinear filtering issues and the parameter settings are simple.

### B. OUTLIER DETECTION AND DOWN-WEIGHT

In order to suppress the large deviation of state estimation results that might be caused by observation or innovation outliers, the outliers need to be detected and downweighted effectively. To detect them, based on the research in [24] and [27], a two-dimensional matrix  $\mathbf{Z}$  that contains the innovation vector and the prediction state vector need to be established as follows

$$\mathbf{Z}_k = \begin{bmatrix} \mathbf{y}_{k-1} - \mathbf{h}(\tilde{\mathbf{x}}_{k-1}) & \mathbf{y}_k - \mathbf{h}(\tilde{\mathbf{x}}_k) \\ \tilde{\mathbf{x}}_{k-1} & \tilde{\mathbf{x}}_k \end{bmatrix}, \quad (28)$$

where the subscripts  $k$  and  $k-1$  represent the time instants;  $\mathbf{y}_{k-1} - \mathbf{h}(\tilde{\mathbf{x}}_{k-1})$  and  $\mathbf{y}_k - \mathbf{h}(\tilde{\mathbf{x}}_k)$  are respectively the innovation vector at time instant  $k-1$  and  $k$ ;  $\tilde{\mathbf{x}}_{k-1}$  and  $\tilde{\mathbf{x}}_k$  indicate the prediction state. Then, the robust projection statistics (PS) estimator can be applied to the matrix  $\mathbf{Z}$  to detect the innovation and observation outliers, the PS estimator is defined as follows [35], [36]

$$PS_j = \max_{\|\boldsymbol{\ell}\|=1} \frac{|\mathbf{l}_j^T \boldsymbol{\ell} - \text{med}_i(\mathbf{l}_i^T \boldsymbol{\ell})|}{1.4826 \text{med}_\kappa |\mathbf{l}_\kappa^T \boldsymbol{\ell} - \text{med}_i(\mathbf{l}_i^T \boldsymbol{\ell})|}, \quad (29)$$

where  $\mathbf{l}_j^T$ ,  $\mathbf{l}_i^T$  and  $\mathbf{l}_\kappa^T$  are respectively the  $j$ th,  $i$ th and  $\kappa$ th row of the matrix  $\mathbf{Z}_k$ , and  $i, j, \kappa = 1, 2, \dots, m+n$ .

Once the PS values of  $\mathbf{Z}_k$  are obtained, the innovation or observation outliers can be detected by comparing the PS values with a given threshold. Due to the PS values of  $\mathbf{Z}_k$  roughly obey the chi-square distribution with 2-degree of freedom [24], therefore, the outlier detection threshold  $\vartheta$  can be set as  $\chi_{v,\beta}^2 = \chi_{2,0.975}^2$ . Then, the outliers with PS values exceed the threshold value can be detected and downweighted via

$$\varpi_i = \min(1, d^2 / PS_i^2), \quad (30)$$

where  $\varpi_i$  represents the down-weight will be utilized in the next part, and the parameter  $d$  is usually set as 1.5.

### C. ESTIMATED STATE UPDATE

The state estimation result against outliers can be obtained by minimizing the following objective function as follows

$$\mathbf{J}(\mathbf{x}) = \sum_{i=1}^{m+n} \varpi_i^2 \boldsymbol{\rho}(r_{S_i}), \quad (31)$$

where  $\varpi_i$  denotes the weight that is calculated by (30);  $r_{S_i} = r_i / (s\varpi_i)$  represents the standardized residual;  $r_i = z_i - \mathbf{c}_i^T \tilde{\mathbf{x}}$  indicates the residual, and  $\mathbf{c}_i^T$  denotes the  $i$ th row vector of  $\mathbf{C}_k$ ;  $s = 1.4826 \cdot b_m \cdot \text{median}_i |r_i|$  represents the robust scale estimate, and the  $b_m$  indicates a correction factor to acquire unbiasedness for a finite sample of size  $m+n$  under the Gaussian distribution;  $\boldsymbol{\rho}(\cdot)$  represents the convex Huber function defined as follows [32]–[34]

$$\boldsymbol{\rho}(r_{S_i}) = \begin{cases} \frac{1}{2} r_{S_i}^2, & \text{for } |r_{S_i}| < \lambda \\ \lambda |r_{S_i}| - \lambda^2/2, & \text{elsewhere,} \end{cases} \quad (32)$$

where  $\lambda$  is usually set as 1.5 to achieve high statistical efficiency.

To minimize the objective function (31), by equating its first partial derivatives with respect to  $\mathbf{x}_k$  to zero, the sufficient and necessary condition for optimality can be obtained

$$\frac{\partial \mathbf{J}(\mathbf{x}_k)}{\partial \mathbf{x}_k} = \sum_{i=1}^{m+n} -\frac{\varpi_i \mathbf{c}_i}{s} \Psi(r_{S_i}) = \mathbf{0}, \quad (33)$$

where  $\Psi(r_{S_i}) = \partial \rho(r_{S_i}) / \partial r_{S_i}$ ,  $\mathbf{c}_i$  represents the  $i$ th column of  $\mathbf{C}_k$ . Then, by dividing and multiplying  $r_{S_i}$  on the both sides of (33), we obtain

$$\mathbf{C}_k^T \boldsymbol{\Omega}(\mathbf{z}_k - \mathbf{C}_k \mathbf{x}_k) = \mathbf{0}, \quad (34)$$

where  $\boldsymbol{\Omega} = \text{diag}\{q(r_{S_i})\}$  and  $q(r_{S_i}) = \Psi(r_{S_i}) / r_{S_i}$ .

**Algorithm 1** Adaptive Robust Cubature Kalman Filter

- 1: Initialization: Set initial values for  $\hat{\mathbf{x}}_0, \hat{\mathbf{P}}_0, \mathbf{Q}_0, \mathbf{R}_0$ , and the total execution time  $N_t$ ;
- 2: Input:  $T_m, E_{fd}, i_R, i_l$  and measurement  $\mathbf{y}_k$ ;
- 3: **while**  $k = 0$  to  $N_t$  **do**
- 4: **step 1:** calculate the predicted state and the corresponding error covariance matrix at time instant  $k$  utilizing the Eqs. (14)-(18)
- 5:  $\tilde{\mathbf{x}}_k \leftarrow \frac{1}{2n} \sum_{i=1}^{2n} \mathbf{X}_{i,k}^*$ ;
- 6:  $\tilde{\mathbf{P}}_k \leftarrow \frac{1}{2n} \sum_{i=1}^{2n} \mathbf{X}_{i,k}^* (\mathbf{X}_{i,k}^*)^T - \tilde{\mathbf{x}}_k \tilde{\mathbf{x}}_k^T + \mathbf{Q}_{k-1}$ ;
- 7: **step 2:** construct the batch-mode regression form and pre-white the noise according to the Eqs. (19)-(27)
- 8:  $\mathbf{z}_k \leftarrow \mathbf{C}_k \mathbf{x}_k + \boldsymbol{\zeta}_k$ ;
- 9: **step 3:** detect the outliers and calculate the down-weights by the Eqs. (28)-(30)
- 10:  $\varpi_i \leftarrow \min(1, d^2 / PS_i^2)$ ;
- 11: **step 4:** update the state estimation according to the Eqs. (31)-(35)
- 12: **while**  $\left\| \hat{\mathbf{x}}_k^{(j+1)} - \hat{\mathbf{x}}_k^{(j)} \right\|_{\infty} > 10^{-2}$  **do**
- 13:  $\hat{\mathbf{x}}_k^{(j+1)} = (\mathbf{C}_k^T \boldsymbol{\Omega}^{(j)} \mathbf{C}_k)^{-1} \mathbf{C}_k^T \boldsymbol{\Omega}^{(j)} \mathbf{z}_k$ ;
- 14: **end while**
- 15: **step 5:** calculate the state estimation error covariance matrix using Eqs. (37)-(39)
- 16: **if**  $\max(PS_i) \leq \chi_{2,0.975}^2$  **then**
- 17:  $\hat{\mathbf{P}}_k \leftarrow \tilde{\mathbf{P}}_k - \mathbf{K}_k \mathbf{P}_{yy,k} \mathbf{K}_k^T$ ;
- 18: **else**
- 19:  $\hat{\mathbf{P}}_k \leftarrow \mu (\mathbf{C}_k^T \mathbf{C}_k)^{-1} (\mathbf{C}_k^T \boldsymbol{\Omega}_{\varpi} \mathbf{C}_k) (\mathbf{C}_k^T \mathbf{C}_k)^{-1}$ ;
- 20: **end if**
- 21: **step 6:** output  $\hat{\mathbf{x}}_k, \hat{\mathbf{P}}_k$  and time instant update
- 22:  $k \leftarrow k + 1$ ;
- 23: **end while**

Then, by utilizing the iterative reweighted least-squares method, the state estimation at the  $j$ th iteration can be calculated via

$$\hat{\mathbf{x}}_k^{(j+1)} = (\mathbf{C}_k^T \boldsymbol{\Omega}^{(j)} \mathbf{C}_k)^{-1} \mathbf{C}_k^T \boldsymbol{\Omega}^{(j)} \mathbf{z}_k. \quad (35)$$

**D. ADAPTIVE UPDATE OF ESTIMATION COVARIANCE MATRIX**

It is worth pointing out that the calculation of the estimation covariance matrix is closely related to the performance of DSE [30]. To enhance the robustness of the proposed method against outliers, by utilizing the total influence function technique in [24], the estimation error covariance matrix can be derived and updated as follows

$$\hat{\mathbf{P}}_k = \mu (\mathbf{C}_k^T \mathbf{C}_k)^{-1} (\mathbf{C}_k^T \boldsymbol{\Omega}_{\varpi} \mathbf{C}_k) (\mathbf{C}_k^T \mathbf{C}_k)^{-1}, \quad (36)$$

where  $\boldsymbol{\Omega}_{\varpi} = \text{diag}\{\varpi_i^2\}$ , the coefficient  $\mu$  is set to be 1.0369 when  $\lambda = 1.5$ .

However, it should be noted that the utilization of (36) might be too conservative, where too much emphasis is placed in accommodating the worst condition (with innovation or observation outliers) at the expense of optimality. In order to improve the robustness of the proposed method without decreasing accuracy, an adaptive strategy is proposed to adjust  $\hat{\mathbf{P}}_k$  in response to the dynamically changing environment

$$\hat{\mathbf{P}}_k = \begin{cases} \tilde{\mathbf{P}}_k - \mathbf{K}_k \mathbf{P}_{yy,k} \mathbf{K}_k^T & \text{if } \max(PS_i) \leq \chi_{2,0.975}^2 \\ \mu (\mathbf{C}_k^T \mathbf{C}_k)^{-1} (\mathbf{C}_k^T \boldsymbol{\Omega}_{\varpi} \mathbf{C}_k) (\mathbf{C}_k^T \mathbf{C}_k)^{-1} & \text{otherwise,} \end{cases} \quad (37)$$

where  $\tilde{\mathbf{P}}_k$  indicates the state prediction error covariance matrix at time instant  $k$ ;  $\chi_{2,(\cdot)}^2$  represents the chi-square distribution with 2 degrees of freedom;  $\chi_{2,0.975}^2$  denotes the value of  $\chi_{2,(\cdot)}^2$  at the significance level of 97.5 %, which is chosen as the outliers detection threshold  $\vartheta$  in this paper;  $\mathbf{P}_{yy,k}$  represents the covariance matrix of the predicted measurement and  $\mathbf{K}_k$  denotes the Kalman gain that can be respectively calculated by

$$\mathbf{P}_{yy,k} = \frac{1}{2n} \sum_{i=1}^{2n} \mathbf{Y}_{i,k} \mathbf{Y}_{i,k}^T - \tilde{\mathbf{y}}_k \tilde{\mathbf{y}}_k^T + \mathbf{R}_k, \quad (38)$$

$$\mathbf{K}_k = \mathbf{P}_{xy,k} \mathbf{P}_{yy,k}^{-1}. \quad (39)$$

Finally, for convenience, the proposed ARCKF approach for power system dynamic state estimation against outliers is fully summarized as Algorithm 1.

*Remark 2:* To deal with the outliers, by utilizing the M-estimation method, a robust Kalman filter was proposed in [32]. Then, following this work, the improved EKF and UKF methods with the similar structure were proposed in [24], [27]. In these methods, the approach in (36) is utilized for updating the estimation error covariance matrix to acquire the strong robustness against outliers. However, it is worth pointing out that the utilization of this method might be too conservative, due to the overemphasis of accommodating the worst condition (with large outliers) at the cost of optimality of the method. Thus, in order to improve the robustness of the proposed method without decreasing the accuracy of state estimation under normal condition, a novel adaptive strategy that makes  $\hat{\mathbf{P}}_k$  adapt to the dynamically changing environment is proposed in (37).

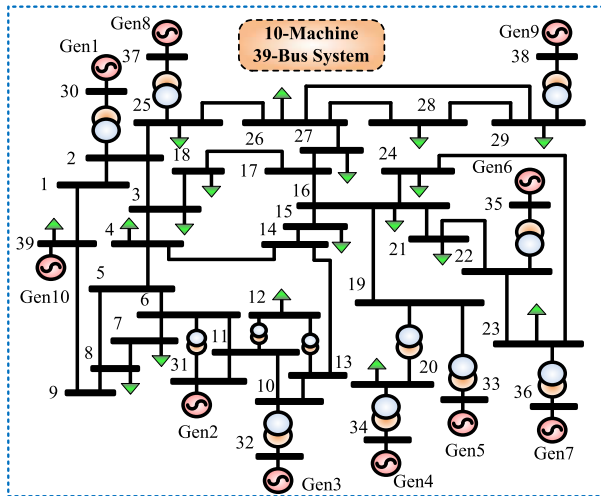


FIGURE 2. Single-line diagram of 10-machine 39-bus test system.

*Remark 3:* With the specific design in (37), while the outliers existing, the state estimation error covariance matrix of  $\hat{P}_k$  will be set as (36) to acquire the strong robustness against outliers and avoid the proposed method divergence; on the other hand, while there are no outliers,  $\hat{P}_k$  will be set as  $\tilde{P}_k - K_k P_{yy,k} K_k^T$ , so that more accurate state estimation results can be achieved.

#### IV. NUMERICAL RESULTS

In this part, extensive simulations have been conducted on the IEEE 10-machine 39-bus system to evaluate the efficiency of the developed ARCKF method. The single-line diagram of this test system is presented in Fig. 2, whose detailed data can be acquired from [37]. Here, the transient stability simulation is performed to generate the simulated PMU measurements and true state variables. The simulation consists of the following steps: a three-phase fault is applied to bus 16 at  $t = 0.5s$  to simulate a large system disturbance, where the fault impedance is 0.001pu and the fault is cleared at  $t = 0.7s$ ; the simulated values of the measurement variables in (4) are corrupted by additive noises to simulate the realistic PMU measurements; note that the sampling frequency of measurements is 50 frames per second. For the state initialization, the steady-state power flow solutions are utilized. In addition, the standard deviations of the measurement and process noise are assumed to be  $10^{-2}$ . More importantly, the conventional UKF method [18], the conventional CKF method [19], and the robust generalized maximum-likelihood unscented Kalman filter approach (GM-UKF) proposed in [27] are also performed, based on the same model and measurements, so as to effectively evaluated the efficacy of the proposed ARCKF method under different case studies. Note that all the following tests are performed on a computer with Intel Core CPU i5-6500 @ 3.2 GHz and 8-GB RAM.

To comprehensively assess the performance of the proposed method against outliers and the computational

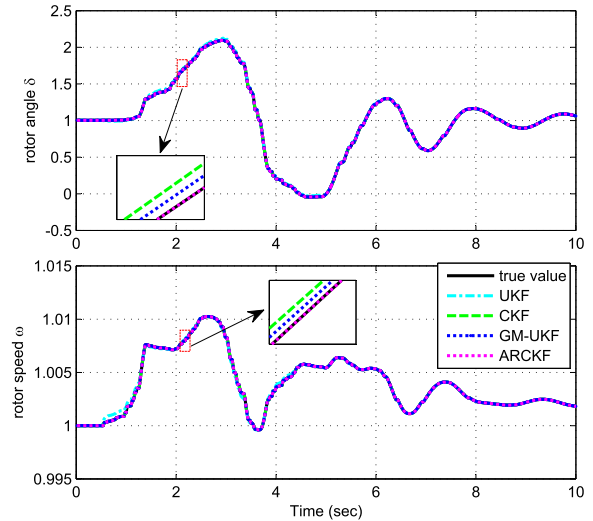


FIGURE 3. Estimated results of  $\delta$  and  $\omega$  for Gen. 8 in the Case Study 1: Normal operating condition.

efficiency, the following five comparative experiments are implemented in the test system:

*Case Study 1:* The conventional UKF method [18], CKF method [19], GM-UKF method [27] and the proposed ARCKF approach are implemented in the test system under the normal condition without innovation and observation outliers, where the state estimation accuracy of each method is investigated and compared in detail.

*Case Study 2:* The performance of all the four discussed approaches with measurements data missing that might be caused by the momentary loss of communication link is investigated and analyzed.

*Case Study 3:* The effects of observation outliers on the state estimation performance of the discussed methods are investigated.

*Case Study 4:* The efficacy of each discussed approach against the innovation outliers that might be caused by the impulsive system process noise or imperfect dynamical model are compared.

*Case Study 5:* The computational efficiency of all the discussed approaches under the case studies 1-4 is investigated and analyzed.

#### A. CASE STUDY 1: NORMAL OPERATING CONDITION

In this case, the performance of the proposed ARCKF approach under normal operating condition is investigated. Specifically, a zero mean Gaussian noise with standard deviation  $10^{-2}$  is assumed for both the process and measurement noise; the initial state estimation error covariance matrix of all the discussed approaches are set to  $10^{-5}I_{4 \times 4}$ . The tracking results of each method for Gen. 8 are shown in Figs. 3 and 4 (actually, the methods have been tested in each generator of the test system, and the simulation results are consistent with the test results of Gen. 8. However, due to the page limit, only the results of Gen. 8 are presented).

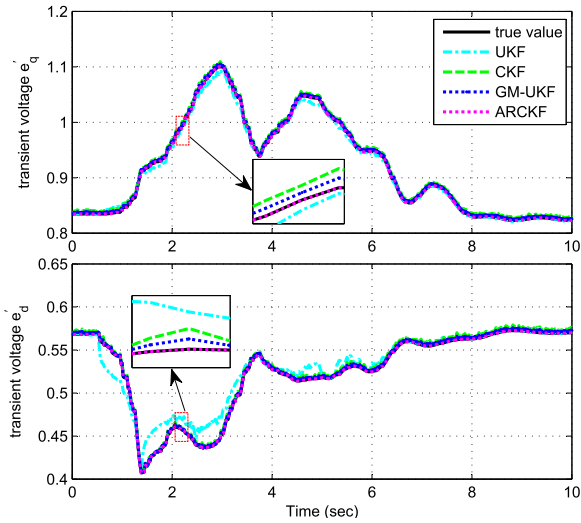


**FIGURE 4.** Estimated results of  $e'_q$  and  $e'_d$  for Gen. 8 in the Case Study 1: Normal operating condition.

It is observed from these figures that all the four discussed approaches can estimate the system states accurately under this ideal condition. However, it should be noticed that the state estimation accuracy of UKF is lower than that of CKF, especially in estimating the state of  $e'_d$ . Similar observations have been noticed in [13]. This is due to the fact that CKF utilizes the spherical-radial cubature rule, which can achieve a higher approximation accuracy of nonlinear system. The GM-Ukf method in [27] can achieve better performance than the conventional UKF and CKF methods, due to its high measurement redundancy and the estimated states can be revised many times by the IRLS method. More importantly, as expected, the proposed ARCKF approach achieves much better performance than the GM-Ukf method, due to its state estimation covariance matrix shown in (37) can be dynamically adjusted to the best status according to the changing environment, which could achieve a high estimation accuracy. These comparisons demonstrate and confirm the superior performance of the proposed method.

**B. CASE STUDY 2: MOMENTARY MEASUREMENT MISSING**

For a practical power system, the momentary measurement data missing may occur due to cyber-attacks, device failures, and communication interruptions, to cite a few [24]. In this case, the measurements  $e_R$  and  $e_I$  of Gen. 8 are assumed to be momentary missing from  $t = 2.2$  s to  $t = 2.3$  s. Thus, the corresponding measurements are unavailable during this time period and their values are set as zero for simulation purpose.

Figs. 5 and 6 display the estimated results of Gen. 8 by using the discussed methods. From these test results, it can be easily found that both the standard UKF and CKF are not capable of tracking system dynamic states while the momentary measurement missing, whose estimated results deviate greatly from their true values. By contrast, the GM-Ukf

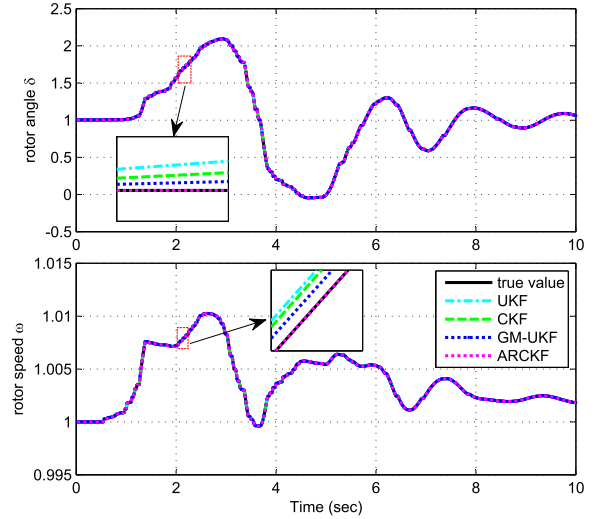


**FIGURE 5.** Estimated results of  $\delta$  and  $\omega$  for Gen. 8 in the Case Study 2 with the measurements missing from  $t = 2.2$  s to  $t = 2.3$  s.

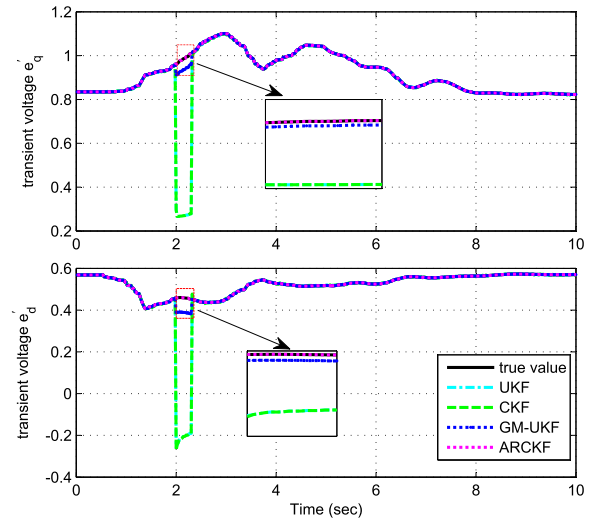


**FIGURE 6.** Estimated results of  $e'_q$  and  $e'_d$  for Gen. 8 in the Case Study 2 with the measurements missing from  $t = 2.2$  s to  $t = 2.3$  s.

method and the proposed ARCKF can suppress the adverse effects of the measurement missing. However, the proposed ARCKF method can achieve a much better statistical efficiency than GM-Ukf [27], which exhibits a stronger robustness.

**C. CASE STUDY 3: OCCURRENCE OF OBSERVATION OUTLIERS**

In this scenario, the effects of observation outliers on the performance of all the discussed methods are investigated and compared, where the measurement  $\omega$  of Gen. 8 is contaminated with gross errors from  $t = 2.2$  s to  $t = 2.4$  s by changing its value to 1.028 pu, simulating an impulsive communication noise.

The estimated results are shown in Figs. 7 and 8. It can be observed that both the standard UKF and CKF are not

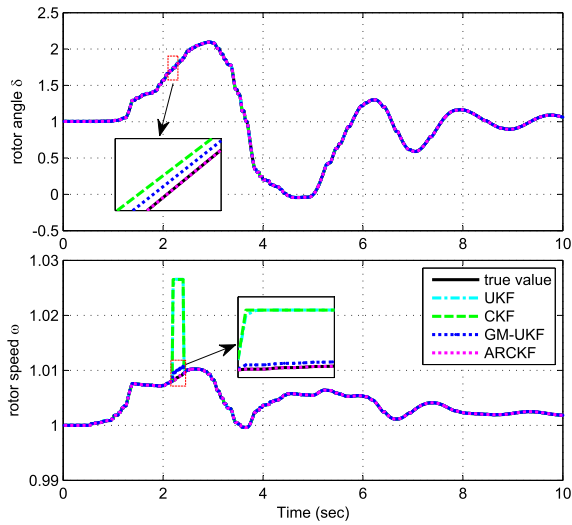


**FIGURE 7.** Estimated results of  $\delta$  and  $\omega$  for Gen. 8 in the Case Study 3, where the measurement  $\omega$  of Gen. 8 is contaminated with gross errors from  $t = 2.2$  s to  $t = 2.4$  s.

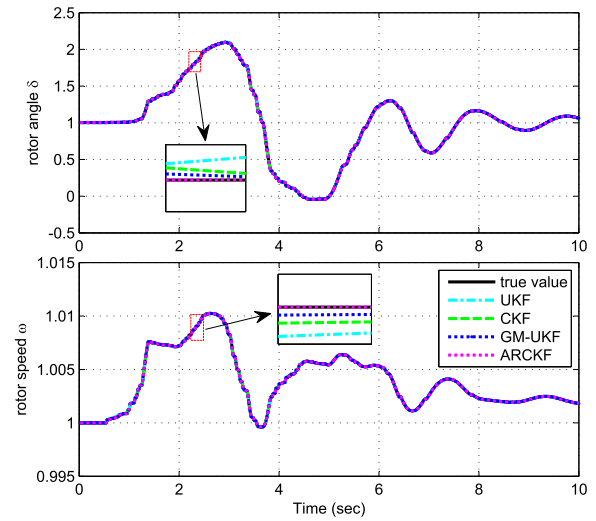


**FIGURE 9.** Estimated results of  $\delta$  and  $\omega$  for Gen. 8 in the Case Study 4, where the predicted value of  $e'_q$  is changed into 0.9 pu from  $t = 2.4$  s to  $t = 2.6$  s.

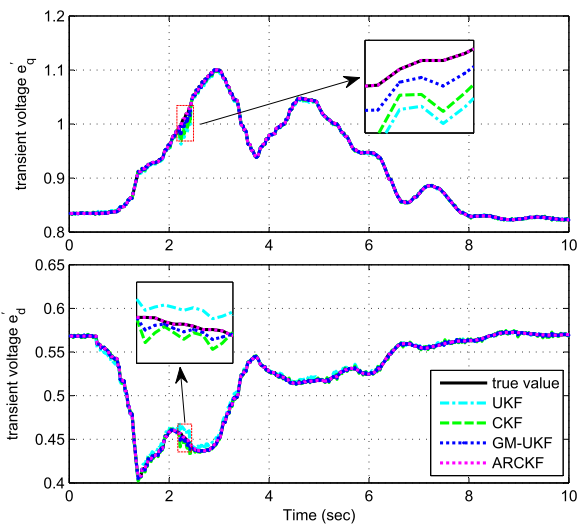


**FIGURE 8.** Estimated results of  $e'_q$  and  $e'_d$  for Gen. 8 in the Case Study 3, where the measurement  $\omega$  of Gen. 8 is contaminated with gross errors from  $t = 2.2$  s to  $t = 2.4$  s.

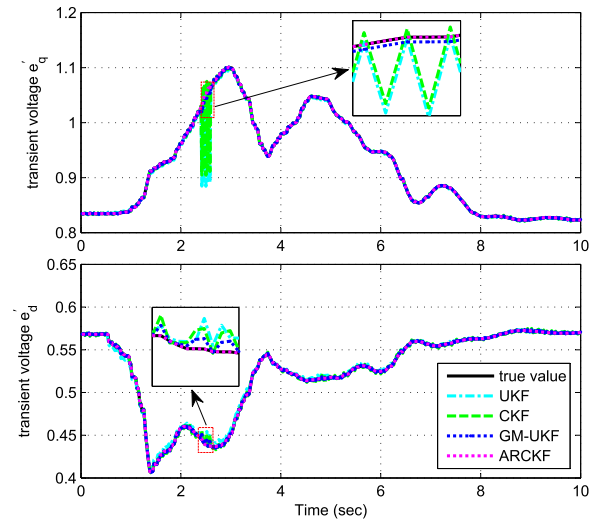


**FIGURE 10.** Estimated results of  $e'_q$  and  $e'_d$  for Gen. 8 in the Case Study 4, where the predicted value of  $e'_q$  is changed into 0.9 pu from  $t = 2.4$  s to  $t = 2.6$  s.

robust to observation outliers, due to the yield significantly biased results at the time while observation outliers occur. In contrast, the GM-UKF approach [27] can achieve more accurate estimation results than the conventional UKF and CKF methods, which can suppress the observation outliers to some extent. However, the GM-UKF [27] can not dynamically adjust the mismatched estimation covariance to the changeable conditions, its estimation errors are still large. By contrast, with the utilization of the GM-estimator and the adaptive state estimation error covariance matrix technique, the proposed method is not only effectively mitigate the adverse effects of the outliers but also achieve a higher estimation accuracy. These comparisons prove the strong robustness of the proposed method against observation outliers.

#### D. CASE STUDY 4: OCCURRENCE OF INNOVATION OUTLIERS

As previously stated, for a practical power system, the innovation outliers are often introduced by the undesirably impulsive system process noise or inaccurate approximation in the state prediction model. To investigate the performance of each discussed approach under this situation, the predicted values of  $e'_q$  are changed to 0.9 pu between  $t = 2.4$  s and  $t = 2.6$  s.

The comparison results are presented in Figs. 9 and 10. As expected, due to the non-robustness of UKF and CKF methods, their performances are degraded sharply when the innovation outliers occurs, yielding unreliable tracking trajectories. Both the proposed ARCKF method and the GM-UKF

**TABLE 1.** Average computing time of the each discussed method.

Cases	CKF	UKF	GM-UKF	ARCKF
Case Study 1	4.12 ms	4.23 ms	7.83 ms	7.90 ms
Case Study 2	4.56 ms	4.61 ms	7.98 ms	8.01 ms
Case Study 3	4.58 ms	4.63 ms	7.99 ms	8.03 ms
Case Study 4	4.59 ms	4.65 ms	8.01 ms	8.06 ms

approach [27] outperform the conventional UKF and CKF approaches, due to their robustness against the innovation outliers. However, ARCKF achieves much better statistical efficiency than the GM-UKF method. These comparisons further prove and confirm the superior performance of the proposed method.

### E. CASE STUDY 5: ASSESSMENT OF COMPUTATIONAL EFFICIENCY

In the design of DSE, computational efficiency is another important factor to be considered, due to a state estimation approach must be fast enough to catch up with the measurement data flow. To verify the applicability of the proposed ARCKF approach to on-line dynamic state estimation with a PMU sampling rate 50 samples/s, its computational efficiency is investigated and compared to that of the GM-UKF, the standard CKF and the UKF in the case studies 1-4. The average computing time of each method required for one iteration is displayed in Table I.

It can be seen from the table that all the four discussed approaches have comparative computational efficiency. Specifically, the CKF method owns the fastest computing speed, followed by the UKF. This is due to the fact that UKF engages one more sigma point for each state, yielding in larger matrices. Both the proposed ARCKF method and GM-UKF approach [27] require more execution time than the standard UKF and CKF methods, due to they contain more equations. However, although the execution time of the proposed ARCKF approach is slightly longer than the other discussed methods, it is still much lower than the PMU sampling period (20ms), demonstrating its ability to track the dynamic system states in real-time.

### V. CONCLUSIONS

This paper proposed an adaptive robust cubature Kalman filter for power system dynamic state estimation against innovation outliers and observation outliers. The method has the following excellent features

- based on the statistical linearization technique, a batch-mode regression form in the framework of CKF was developed by processing the measurement data and predicted state information simultaneously, yielding an enhanced observation data redundancy. This redundancy is necessary and important for the designed dynamic state estimator to suppress the innovation outliers and observation outliers;

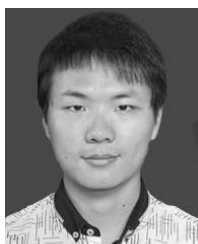
- the innovation and observation outliers can be detected and downweighted by utilizing the robust projection statistics, based on which, the adverse effects of the innovation and observation outliers can be effectively suppressed by solving the robust GM-estimator;
- an adaptive strategy that makes the state estimation error covariance matrix adapt to the dynamically changing environment was designed, which can further enhance the robustness of the proposed method without decreasing the accuracy of state estimation under normal condition.

Extensive simulation tests carried out on the IEEE New England 10-machine and 39-bus test system under various operating conditions demonstrated the effectiveness and robustness of the proposed method.

### REFERENCES

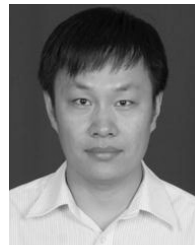
- [1] W. Li, L. Vanfretti, and J. H. Chow, "Pseudo-dynamic network modeling for PMU-based state estimation of hybrid AC/DC grids," *IEEE Access*, vol. 6, pp. 4006–4016, 2017.
- [2] L. Hu, Z. Wang, I. Rahman, and X. Liu, "A constrained optimization approach to dynamic state estimation for power systems including PMU and missing measurements," *IEEE Trans. Control Syst. Technol.*, vol. 24, no. 2, pp. 703–710, Mar. 2016.
- [3] H. Karimipour and V. Dinavahi, "Robust massively parallel dynamic state estimation of power systems against cyber-attack," *IEEE Access*, vol. 6, pp. 2984–2995, 2017.
- [4] R. C. Magaña, A. Medina, V. Dinavahi, and A. Ramos-Paz, "Time-domain power quality state estimation based on Kalman filter using parallel computing on graphics processing units," *IEEE Access*, vol. 6, pp. 21152–21163, 2018.
- [5] H. Karimipour and V. Dinavahi, "Parallel relaxation-based joint dynamic state estimation of large-scale power systems," *IET Gener., Transmiss. Distrib.*, vol. 10, no. 2, pp. 452–459, Feb. 2016.
- [6] Y. Cui, R. G. Kavasseri, and S. M. Brahma, "Dynamic state estimation assisted out-of-step detection for generators using angular difference," *IEEE Trans. Power Del.*, vol. 32, no. 3, pp. 1441–1449, Jun. 2017.
- [7] Y. Liu, A. P. S. Meliopoulos, R. Fan, L. Sun, and Z. Tan, "Dynamic state estimation based protection on series compensated transmission lines," *IEEE Trans. Power Del.*, vol. 32, no. 5, pp. 2199–2209, Oct. 2017.
- [8] M. M. Rana, L. Li, S. W. Su, and B. J. Choi, "Modelling the interconnected synchronous generators and its state estimations," *IEEE Access*, vol. 6, pp. 36198–36207, 2018.
- [9] Z. Huang, K. Schneider, and J. Nieplocha, "Feasibility studies of applying Kalman filter techniques to power system dynamic state estimation," in *Proc. 8th Int. Power Eng. Conf.*, Singapore, Dec. 2007, pp. 376–382.
- [10] L. Fan and Y. Wehbe, "Extended Kalman filtering based real-time dynamic state and parameter estimation using PMU data," *Electr. Power Syst. Res.*, vol. 103, pp. 168–177, Oct. 2013.
- [11] E. Ghahremani and I. Kamwa, "Dynamic state estimation in power system by applying the extended Kalman filter with unknown inputs to phasor measurements," *IEEE Trans. Power Syst.*, vol. 26, no. 4, pp. 2556–2566, Nov. 2011.
- [12] E. Ghahremani and I. Kamwa, "Local and wide-area PMU-based decentralized dynamic state estimation in multi-machine power systems," *IEEE Trans. Power Syst.*, vol. 31, no. 1, pp. 547–562, Jan. 2016.
- [13] I. Arasaratnam and S. Haykin, "Cubature Kalman filters," *IEEE Trans. Autom. Control*, vol. 54, no. 6, pp. 1254–1269, Jun. 2009.
- [14] S. Akhlaghi, N. Zhou, and Z. Huang, "A multi-step adaptive interpolation approach to mitigating the impact of nonlinearity on dynamic state estimation," *IEEE Trans. Power Syst.*, vol. 9, no. 4, pp. 3102–3111, Jul. 2018.
- [15] N. Zhou, D. Meng, and S. Lu, "Estimation of the dynamic states of synchronous machines using an extended particle filter," *IEEE Trans. Power Syst.*, vol. 28, no. 4, pp. 4152–4161, Nov. 2013.
- [16] A. K. Singh and B. C. Pal, "Decentralized dynamic state estimation in power systems using unscented transformation," *IEEE Trans. Power Syst.*, vol. 29, no. 2, pp. 794–804, Mar. 2014.

- [17] G. Anagnostou and B. C. Pal, "Derivative-free Kalman filtering based approaches to dynamic state estimation for power systems with unknown inputs," *IEEE Trans. Power Syst.*, vol. 33, no. 1, pp. 116–130, Jan. 2018.
- [18] G. Valverde and V. Terzija, "Unscented Kalman filter for power system dynamic state estimation," *IET Generat., Transmiss. Distrib.*, vol. 5, no. 1, pp. 29–37, Jan. 2011.
- [19] A. Sharma, S. C. Srivastava, and S. Chakrabarti, "A cubature Kalman filter based power system dynamic state estimator," *IEEE Trans. Instrum. Meas.*, vol. 66, no. 8, pp. 2036–2045, Aug. 2017.
- [20] M. A. Kardan, M. H. Asemani, A. Khayatian, N. Vafamand, M. H. Khooban, T. Dragičević, and F. Blaabjerg, "Improved stabilization of nonlinear DC microgrids: Cubature Kalman filter approach," *IEEE Trans. Ind. Appl.*, vol. 54, no. 5, pp. 5104–5112, Sep. 2018.
- [21] D. Simon, *Optimal State Estimation*. Hoboken, NJ, USA: Wiley, 2006.
- [22] K. Zhou, J. C. Doyle, and K. Glover, *Robust and Optimal Control*. Upper Saddle River, NJ, USA: Prentice-Hall, 1996.
- [23] M. Asprou and E. Kyriakides, "Identification and estimation of erroneous transmission line parameters using PMU measurements," *IEEE Trans. Power Del.*, vol. 32, no. 6, pp. 2510–2519, Dec. 2017.
- [24] J. Zhao, M. Netto, and L. Mili, "A robust iterated extended Kalman filter for power system dynamic state estimation," *IEEE Trans. Power Syst.*, vol. 32, no. 4, pp. 3205–3216, Jul. 2017.
- [25] K. D. Jones, A. Pal, and J. S. Thorp, "Methodology for performing synchrophasor data conditioning and validation," *IEEE Trans. Power Syst.*, vol. 30, no. 3, pp. 1121–1130, May 2015.
- [26] A. Rouhani and A. Abur, "Linear phasor estimator assisted dynamic state estimation," *IEEE Trans. Smart Grid*, vol. 9, no. 1, pp. 211–219, Jan. 2018.
- [27] J. Zhao and L. Mili, "Robust unscented Kalman filter for power system dynamic state estimation with unknown noise statistics," *IEEE Trans. Smart Grid*, vol. 10, no. 2, pp. 1215–1224, Mar. 2019.
- [28] Y. Li, J. Li, J. Qi, and L. Chen, "Robust cubature Kalman filter for dynamic state estimation of synchronous machines under unknown measurement noise statistics," *IEEE Access*, vol. 7, pp. 29139–29148, 2019.
- [29] P. Kundur, *Power System Stability and Control*. New York, NY, USA: McGraw-Hill, 1994.
- [30] Y. Wang, Y. Sun, V. Dinavahi, K. Wang, and D. Nan, "Robust dynamic state estimation of power systems with model uncertainties based on adaptive unscented  $H_\infty$  filter," *IET Gener., Transmiss. Distrib.*, vol. 13, no. 12, pp. 2455–2463, Jun. 2019. doi: 10.1049/iet-gtd.2019.0031.
- [31] T. Lefebvre, H. Bruyninckx, and J. De Schuller, "Comment on 'A new method for the nonlinear transformation of means and covariances in filters and estimators' [with authors' reply]," *IEEE Trans. Autom. Control*, vol. 47, no. 8, pp. 1406–1408, Aug. 2002.
- [32] S. C. Chan, Z. G. Zhang, and K. W. Tse, "A new robust Kalman filter algorithm under outliers and system uncertainties," in *Proc. IEEE Int. Symp. Circuits Syst. (ISCAS)*, May 2005, pp. 4317–4320.
- [33] C. Zhang, R. Zhi, T. Li, and J. Corchado, "Adaptive M-estimation for robust cubature Kalman filtering," in *Proc. Sensor Signal Process. Defence (SSPD)*, Edinburgh, U.K., Sep. 2016, pp. 1–5.
- [34] T.-C. Li, J.-Y. Su, W. Liu, and J. M. Corchado, "Approximate Gaussian conjugacy: Parametric recursive filtering under nonlinearity, multimodality, uncertainty, and constraint, and beyond," *Frontiers Inf. Technol. Electron. Eng.*, vol. 18, no. 12, pp. 1913–1939, Dec. 2017.
- [35] W. A. Stahel, "Breakdown of covariance estimators," Fachgruppe für Statistik, ETH, Zürich, Germany, Res. Rep. 31, 1981.
- [36] D. L. Donoho, "Breakdown properties of multivariate location estimators," Ph.D. dissertation, Harvard Univ., Cambridge, MA, USA, 1982.
- [37] M. A. Pai, *Energy Function Analysis for Power System Stability*. New York, NY, USA: Springer, 1989.



**YI WANG** received the B.S. degree from the Luoyang Institute of Science and Technology, Luoyang, China, in 2014. He is currently pursuing the Ph.D. degree in electrical engineering with Hohai University, Nanjing, China. He is studying at the University of Alberta, Canada, as a joint Ph.D. student, from 2018 to 2019.

His research interests include theoretical and algorithmic studies in power system estimation, parameters identification, power system dynamics, signal processing, and cyber security.

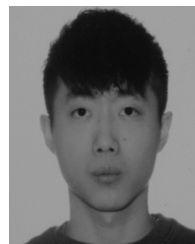


**YONGHUI SUN** (M'16) received the Ph.D. degree from the City University of Hong Kong, Hong Kong, in 2010. He is currently a Professor with the College of Energy and Electrical Engineering, Hohai University, Nanjing, China. He has authored more than 60 papers in refereed international journals. His research interests include stability analysis and control of power systems, optimal planning and operation of integrated energy systems, optimization algorithms, and data analysis.

Dr. Sun was a recipient of the First Award of Jiangsu Provincial Progress in Science and Technology, in 2010, as the Fourth Project Member, and he is an Active Reviewer for many international journals.



**VENKATA DINAVAH** (S'94–M'00–SM'08) received the B.Eng. degree in electrical engineering from the Visveswaraya National Institute of Technology (VNIT), Nagpur, India, in 1993, the M.Tech. degree in electrical engineering from the Indian Institute of Technology (IIT) Kanpur, Kanpur, India, in 1996, and the Ph.D. degree in electrical and computer engineering from the University of Toronto, Toronto, ON, Canada, in 2000. He is currently a Professor with the Department of Electrical and Computer engineering, University of Alberta, Edmonton, AB, Canada. His research interests include real-time simulation of power systems and power electronic systems, electromagnetic transients, device-level modeling, large-scale systems, and parallel and distributed computing.



**SHIQI CAO** (S'19) received the B.Eng. degree in electrical engineering and automation from the East China University of Science and Technology, China, in 2015, and the M.Eng. degree in power system from Western University, Canada, in 2017. He is currently pursuing the Ph.D. degree in electrical and computer engineering with the University of Alberta, Canada. His research interests include transient stability analysis, power electronics, and field programmable gate arrays.



**DONGCHEN HOU** received the B.S. degree from the College of Electric Power, North China University of Water Resources and Electric Power, Henan, China, in 2017. He is currently pursuing the Ph.D. degree with the College of Energy and Electrical Engineering, Hohai University, Nanjing, China.

His research interests include the theory and algorithms of power system state estimation, attack identification, robust state estimation, and Kalman filter.

• • •